Chapter 31
Monitoring Marsh Dynamics Through Remote Sensing

Ricardo Díaz-Delgado, David Aragonés, Iban Ameztoy, and Javier Bustamante

The Value of Remote Sensing Images

The first synoptic images from space were provided by TIROS spacecraft with a video camera onboard in 1960 (Susskind *et al.* 1984), these images revealed a huge spheroid fully covered by oceans and clouds. There was still a long way to travel from simply picturing Earth to the current technological achievements of remote sensing science. However, the main scientific purposes of using remote sensing images have been maintained since those days. The very earliest uses of remote sensing are now much more focused and widespread, and often driven by military objectives. Indeed, remote sensing owes its rapid development almost exclusively to military initiatives (Barret and Curtis 1999). From a military perspective, targets should be differentiated as accurately as possible, and this requirement has resulted in the increased spatial resolution of remote sensors. Spectral resolution – the number of sensor bands imaging at different wavelengths – has been cultivated to help discriminate between false positives and true targets.

Space technology has also played an essential role in improving the potential of remote sensing – mostly by enhancing satellite platform designs, accurate orbiting and the launch of more satellites.

However, it was at the beginning of the 1970s when a new concept for remote sensing was introduced and that the new technology drifted towards a more applied discipline: Earth Observation Systems (EOS). While hundreds of satellites were launched for telecommunication, military uses or spatial prospecting, a few were also designed simply to monitor the Earth surface under the EOS concept. This new

R. Díaz-Delgado (✉)
Head of Landscape & Remote Sensing Monitoring, Doñana Biological Station-CSIC, c/Américo Vespucio s/n. Isla de la Cartuja, Sevilla, 41092, Spain
e-mail: rdiaz@ebd.csic.es

D. Aragonés, I. Ameztoy and J. Bustamante
Remote Sensing & GIS Laboratory (LAST), Doñana Biological Station-CSIC, c/Américo Vespucio s/n. Isla de la Cartuja, Sevilla, 41092, Spain

C. Hurford et al. (eds.), *Conservation Monitoring in Freshwater Habitats: A Practical Guide and Case Studies*, DOI 10.1007/978-1-4020-9278-7_31,

generation of Earth sentinels aimed to systematically capture images from all over the world. The first two missions with this aim were the NOAA-AVHRR (Advanced Very High Resolution Radiometer) mission and the Landsat mission (originally named ERTS from Earth Resources Technology Satellite). The former was basically designed for oceanography and meteorology and launched in 1979. The latter, with the MSS (Multi-Scanner Sensor) onboard, was launched in 1972 and designed primarily to image Earth land cover. Both missions are ongoing and carry completely new sensors (Table 31.1). The main differences between the two are the spatial and temporal resolutions. NOAA-AVHRR was able to acquire 2,580 km swath of 1.1 × 1.1 km^2 pixel size images while Landsat captured 185 × 185 km^2 scenes of 59 × 79 m^2 pixel size images. NOAA-AVHRR missions have increased our knowledge of weather patterns, sea surface temperature, global vegetation dynamics, wildfire monitoring, snow cover, etc., whereas Landsat missions have contributed more to understanding land cover dynamics and change, such as deforestation, flood mapping, fire scar and fire risk mapping.

Since 2000, hundreds of Earth Observation Systems have been launched with significantly improved spatial resolutions of up to 60 cm (Quickbird panchromatic), improved spectral resolution (prototype hyperspectral missions are already providing 200 bands images such as Hyperion), improved radiometric resolution (up to 1,024 bits such as MODIS Terra/Aqua) and improved temporal resolution (geostationary satellites such as MSG-2 provide images every 15 min). These technological achievements have successfully contributed to the development of remote sensing, and forestry, geology, agriculture, urban planning, biology, ecology, climatology, geography, archaeology and hydrology, are just some of the disciplines that have benefited from the use of remote sensing images.

However, there is also an added value attached to the use of remote sensing images. Some sensors have been capturing images of the same locations for 36 years, giving end-users a powerful multi-temporal time series of images that can be acquired retrospectively to study any natural process and its dynamics, as well as historical

Table 31.1 Comparison of the spectral, temporal and spatial resolutions of Landsat MSS, TM and NOAA-AVHRR imagery. Modified from Ozesmi and Bauer (2002)

Resolution	Landsat MSS	Landsat TM	AVHRR
Band 1		0.45–0.52	0.58–0.68
Band 2		0.52–0.60	0.72–1.10
Band 3		0.63–0.69	3.55–3.93
Band 4	0.5–0.6	0.76–0.90	0.77–0.86
Band 5	0.6–0.7	1.55–1.75	11.5–12.5
Band 6	0.7–0.8	10.4–12.5	
Band 7	0.8–1.1	2.08–2.35	
Radiometric (bits)	64	256	1,024
Temporal	18 days	16 days	12 h
Spatial	59 × 69 m^2	30 m, 120 m TM	1.1 km at nadir
First launched	1972	1982	1979

changes, by means of digital image analysis. Hopefully, many of the historical sensors will remain active so that we can expand these time series into the future.

Remote Sensing Limitations

Although many studies provide evidence to support the use of remote sensing images for mapping land use and land cover, as well as the different structural and biophysical parameters characterising them, we are also aware of many limitations. These restrictions increase when our aim is to analyse a time series of images, for example:

1. High resolution satellite images are expensive
2. There are intellectual property restrictions
3. There is limited availability and usability of optical images as a result of:
   - Cloud cover
   - Sensor or acquisition failure
   - Acquisition planning and scheduling
   - Mission continuity
4. The need for geometric and radiometric consistency among scenes to allow consistent removal of atmospheric effects
5. The restricted spectral range of nominal bands
6. Insufficient revisiting time
7. The need for ground-truth data (data collected in the field)
8. Extensive data processing
9. Computer limitations
10. Subscription rates for future image acquisitions

The following example illustrates how these limitations can impact on a project. In 2002, the Remote Sensing & GIS Laboratory (LAST-EBD) from Doñana Biological Station had the opportunity to acquire a long time-series of Landsat images (MSS, TM and ETM+) for the Doñana region (Landsat scene 202/34). We ordered all the available scenes for this path and row through the European distributor Eurimage. At that time, 239 scenes were available, covering the period from 1975 to 2001. The MSS scenes cost 200 € each, while TM and ETM+ were on special offer at 700 € each, giving a total cost of 133,000 €. From the available dates we requested, about 30 scenes were under cloud cover and another 56 were rejected due to different acquisition failures. We then entered a contract for a periodical research subscription for future scene acquisitions, priced at 500 € per image. To date, LAST-EBD has been under subscription for 5 years, but in 2004 the subscription rules changed. Initially, there was a chance to replace up to two cloud-covered images with new requests. Nowadays, there is no option to reject fully cloud-covered scenes despite the images being totally useless.

Before processing the time-series, we set up a protocol that included metadata retrieval, geometric correction, co-registration, radiometric correction and normalisation

and backup for every scene. This process can be time consuming (up to 4 h per image) but recently we have reduced this by up to 1 h per image.

One of the first applications of the Landsat time series was to map flooding levels in the Doñana marshland and reconstruct the historic flooding regime, looking at both temporal and spatial patterns. After several trials to identify true wetland, cross-validated with ground-truth data, TM band 5 (1.55–1.75 m) was selected as the best variable to mask water bodies by simple thresholding. We then computed flood masks, i.e. binary images of flooded pixels (value 1) and non-flooded pixels (value 0) for every single date and calculated the hydroperiod (duration of flooding per hydrological cycle). However, the unavailability of certain scenes prevented us from estimating this valuable variable for every cycle. The secondary goals of the research project were to map aquatic vegetation tightly linked to the hydroperiod and then to analyse plant dynamics and changing trends. Different approaches have been trialled to this end, but with no satisfactory results to date, mostly due to the lack of thin spectral bands in the short wave infrared region that might help to discriminate the critical plant species.

In 1999, Landsat 7 was launched with the introduction of the ETM+ sensor, an Enhanced Thematic Mapper that added a new panchromatic band of 15 × 15 m^2 pixel size and increased the thermal band spatial resolution up to 60 m. Due to its longevity, the Landsat mission has suffered many major setbacks in its time, including a failure to reach orbit (Landsat 6 in 1993) and unexpected sensor malfunction, such as the Scan Line Corrector failure of ETM+ in 2003 that yields a zigzag pattern across the satellite ground track. However, astonishingly, Landsat 5, which was launched in 1984, is still orbiting and has been reprogrammed to capture new images up to the present time. Most recently, in April 2008, USGS (US Geological Survey) who operate the Landsat mission, announced plans to provide all archived Landsat scenes at no charge to users. Today, the historical dataset for any place in the world can be requested and downloaded from Glovis (http://glovis.usgs.gov) or Earth Explorer (http://earthexplorer.usgs.gov).

As such, many of the cited constraints associated with using remote sensing as the main tool for long-term monitoring have been resolved (within reason), increasing its suitability for monitoring large or inaccessible wetlands.

Remote Sensing for Wetlands

The first remote sensing applications targeting wetlands dealt with basic delineation of wetland boundaries. In addition to eventual flood and floodplain mapping, wetlands have been mapped and inventoried with remote sensing images since the 1970s. Remote sensing appears to be the best tool for mapping large and relatively inaccessible areas (Engman and Gurney 1991). The rationale behind the remote sensing approach to delimiting water bodies relies on the fact that water has a relatively low reflectance, especially in the near-infrared region, from 0.7 to 3.0 m (Gardiner and Díaz-Delgado 2007). Therefore, the accuracy of detection is based

on the reliable identification of water and the spatial resolution of the sensor. Interestingly, cloud shadows, dark soils, closed canopy forests and urban areas may show similar reflectance values. Image interpretation was used as mapping tool long before the development of digital image analysis techniques. The human eye may easily integrate information from colour, texture, intensity and contextual characteristics allowing quick delineation of water bodies despite being shallow or deep, turbid or pristine, plant covered or bare water. However, this approach is always subject to individual interpretation and can be very time-consuming. Digital image analysis offers, through the application of validated algorithms and classification rules, an objective way to proceed with a multi-temporal series of images.

Long-Term Monitoring of Doñana Marshland Through Remote Sensing

Doñana marshes occupy almost 500 km^2 at the mouth of the Guadalquivir River (SW Spain). Protected as a National Park since 1968, it is the largest wetland in Europe and vast numbers of waterfowl breed or use the marshes as a stop-over site during migration. Natural inundation takes place between October and March, mostly fed by rain in the drainage watershed. Since an artificial levée was built in 1984, tidal influence is no longer a significant factor. The levée retains water inside the marsh for as long a time as possible, operating as a dump and preventing saline water from entering. In 1998, toxic runoff from the Aználcollar mine into the Guadiamar River made it necessary to dam the affected river to avoid a pollution of the Doñana marshlands, which caused an artificial increase of the marshland hydroperiod. As such, the historical inundation regime has changed dramatically as a consequence of management decisions. Today, Doñana encompasses an ambitious restoration project called Doñana 2005, which aims to restore the natural inundation process by applying widely accepted decisions based on data gathered over the past 10 years on a point station basis.

In this context, more than ever, it is necessary to know the historical inundation patterns, either spatial or temporal, and their relationships with natural variability and human modifications. For many years, details of the inundation process, such as inter-annual and seasonal variation, both spatial and temporal, as well as the influence of human transformations have been required by decision-makers in order to apply a scientific-based or adaptive management regime to Doñana marshes. To date, the hydrological management has been conducted on an "event-reaction" basis, which has led to temporary solutions eventually becoming a part of new problems. Hence, to date, the long-term monitoring protocols for Doñana wetlands include hydroperiod mapping, i.e. the duration of flooding within the hydrological cycle; spatially explicit flood mapping, i.e. to reconstruct the flooding regime; water turbidity; water depth and water temperature. Remote sensing is the main tool used for monitoring these protocols.

Flood Mapping, Hydroperiod and Flooding Regime

As stated previously, water bodies have low reflectivity, especially in Near Infrared and Mid Infrared bands (bands 4, 5 and 7 of TM and ETM+), and several procedures have been developed to identify flooded areas based on the low reflectivity of water in these spectral regions. Some indices have been proposed to automatically determine the inundation level in Landsat scenes. Ángel-Martínez (1994) suggests the CEDEX index to discriminate continental waters:

CEDEX = (TM4/TM3) – (TM4/TM5)

Where TM4 accounts for either TM or ETM band 4. According to Castaño *et al.* (1999) CEDEX values below 0.4 are inundated areas. Domínguez Gómez (2002) suggests the Normalized Difference Water Index (McFeeters 1996) as being useful to discriminate oligotrophic waters:

NDWI = (TM2 – TM4) / (TM1 + TM4)

Domínguez Gómez (2002) argues that the NDWI fails when applied to images collected by the airborne ATM-Daedalus sensor and suggests that it is better to apply simple band thresholding (density slicing) on the B4 histogram. Kyu-Shun *et al.* (2001), working in wetlands with different turbidity levels, show that TM5 is less sensitive to sediment charged waters and therefore the best to delineate the borders between water and soil in turbid waters.

Finally, several authors have argued that the third component of Tasseled Cap transformation for TM (Crist and Cicone 1984; Baker *et al.* 2006), known as 'Wetness', is tightly related to soil wetness. We also compute this index with the coefficients for Landsat 5 and 7 for reflectivity values in order to evaluate the capability for discriminating inundation levels.

Doñana marshlands are highly variable. They may appear as dry soil in summer, as bare water pools during the flooding season, or as pools densely covered by emergent and floating plants; in both cases with patchy turbidity patterns due to differences in suspended sediment concentrations (Fig. 31.1). In order to capture this variability, we carried out seven ground-truth sampling campaigns simultaneously with the acquisition of six Landsat scenes (4 TM and 2 ETM+).

Several transects were located across heterogeneous inundated areas and every 60 m we recorded information on water turbidity (measured in NTU with a nephelometric turbidimeter), depth, bare ground cover, plant cover, open water cover, dominant and most abundant plant species and inundation level.

Among several bands and radiometric indices, band TM5 was selected as the best flooding level discriminator for all of the cases. Single image slicing using a regression tree technique enabled us to map four flooding levels (dry soil, wet, damp and inundated). Regression trees identify threshold values to assign spectral classes to thematic categories. Subsequent grouping of the dry soil and wet pixels, and damp soil and inundated pixels, allowed us to automatically produce flooding inundation masks for every available Landsat scene covering the period 1984–2007 (Fig. 31.2). A similar process was applied retrospectively to band 7 of the Landsat MSS time series of images, which covered the period 1975–1984.

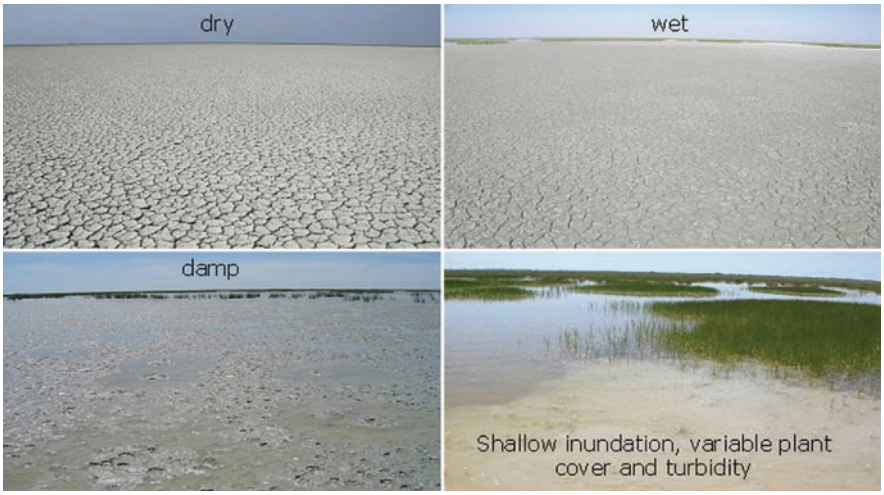

Fig. 31.1 Pictures showing the variability of Doñana marshlands

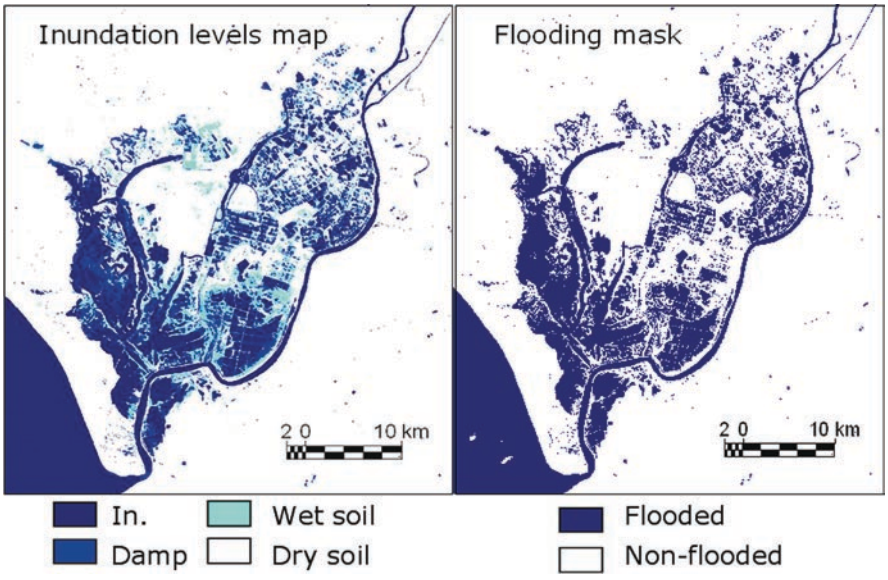

Fig. 31.2 An example of the inundation levels map and flooding mask for the same date image, 7th January 2002. Note that the dry and wet soils are classified as non-flooded areas in the flooding mask

We estimated the hydroperiod for the whole time series by applying two different approaches to the masks. The first method provides a synthetic image in which every pixel shows the number of days it remained inundated over a complete hydrological cycle (from 1st September to 31st August). This method assumes that flooding has been maintained between two consecutive scenes if flooding has been detected in both. This first approach consisted of assigning the cycle day number (number corresponding to image date being 1st September valued as 1 and 31st August valued 365) to flooded pixels of every inundation mask.

Thus, final images give information on the number of days a pixel remained inundated per cycle, named annual hydroperiod (Díaz-Delgado *et al.* 2006a). We also generated decadal hydroperiod composites by adding every available date per month and subsequently averaging the results per decade. This latter method was designed to allow inter-decadal comparison after important transformations in the marshland, while the former aims to detect quantitative local changes in hydroperiod trends when subjected to natural variability and human transformations (Fig. 31.3). Both automatic mapping procedures are also systematically applied to the new acquired scenes by Landsat TM and ETM+.

Water Turbidity and Depth

Turbidity is a measure of how much of the light travelling through water is scattered by suspended particles. The scattering of light increases with increasing suspended

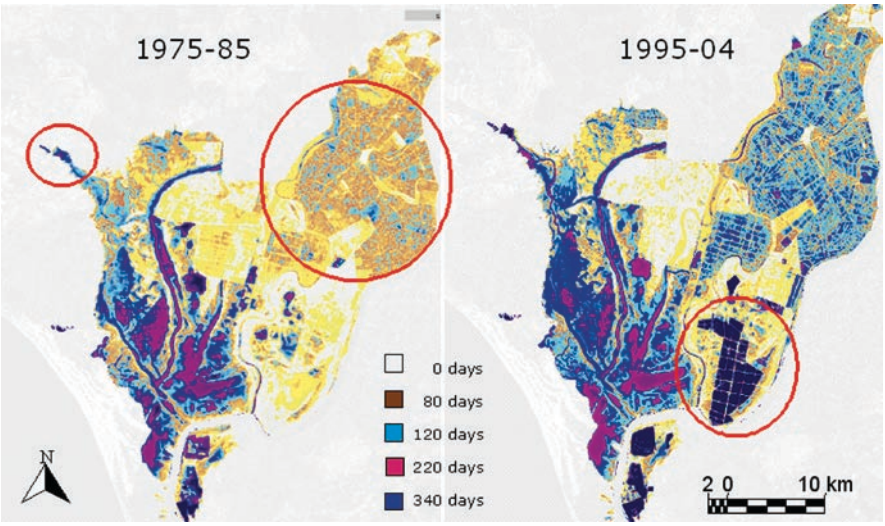

Fig. 31.3 A comparison of the decadal hydroperiod in the 1975–1985 and 1995–2004 decades. The legend shows the average number of days per decade inundated (from 0 to 365). *Red circles* highlight large differences in the hydroperiod between decades, such as the Veta la Palma fisheries, rice fields and main water income areas

solid and plankton content, i.e. turbidity is a tight surrogate of SSC (Suspended Sediments Concentration) and chlorophyll content.

In order to map the turbidity and depth of Doñana marshlands we fit, in a step-by-step mode, a generalized additive model (GAM) to ground-truth data by using the best Landsat sensor bands and indices as predictors (Bustamante *et al.* 2009). The best GAM model selected with the step-by-step procedure included bands TM3, TM5 and the ratio B1/B4. The model indicated a positive curvilinear relationship with TM3, a negative curvilinear relationship with TM5 and a negative linear relationship with the ratio B1/B4. The model explained 40% of the variance in turbidity (Fig. 31.4a).

Water turbidity is best estimated in situations where bottom soil reflectance and aquatic vegetation do not interfere, but it is still possible to build a predictive model for situations like those of the Doñana marshes – with shallow waters and abundant aquatic vegetation

Unlike for turbidity, the best predictors bands for the depth model were TM1, TM5, the ratio TM2/TM4, and bottom soil reflectance in band TM4 (from an image in September, when the marsh is completely dry) and the ratio between the B4 reflectance and the B4 reflectance for the same pixel in September. As expected, we found that band TM1 was the most informative wavelength as it is inversely related to depth. The model explained 75.42% of the variance. Once applied to the images we produced more than 240 maps of the water depth in Doñana marshlands showing the historical changes in its bathymetric characteristics (Fig. 31.4b).

On the basis of these results and newly available image acquisitions, we are currently monitoring water turbidity and depth by producing quantitative maps and identifying the main trends for both parameters (Díaz-Delgado *et al.* 2006b).

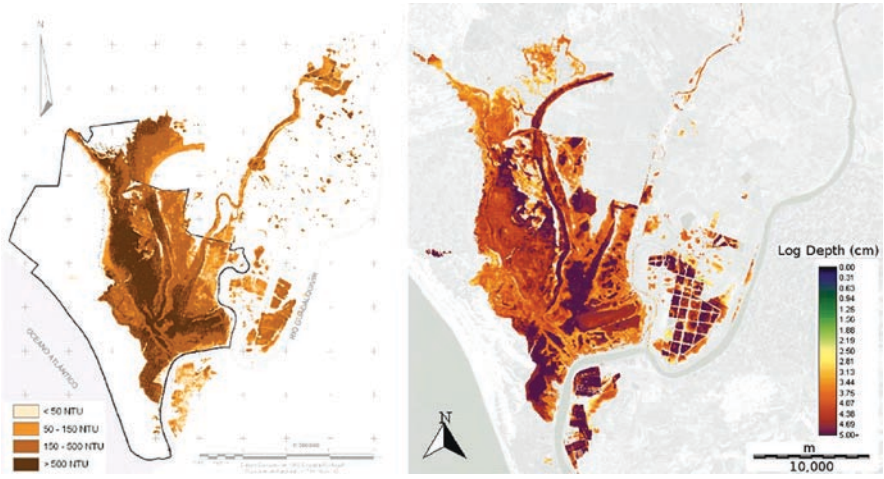

Fig. 31.4 (**a**) A reclassified water turbidity map of the Doñana marshes for the Landsat TM image of 14th January 1990. (**b**) The water depth map of the flooded area in the Doñana marshes in logarithmic scale for the Landsat TM image of 25th March 2004

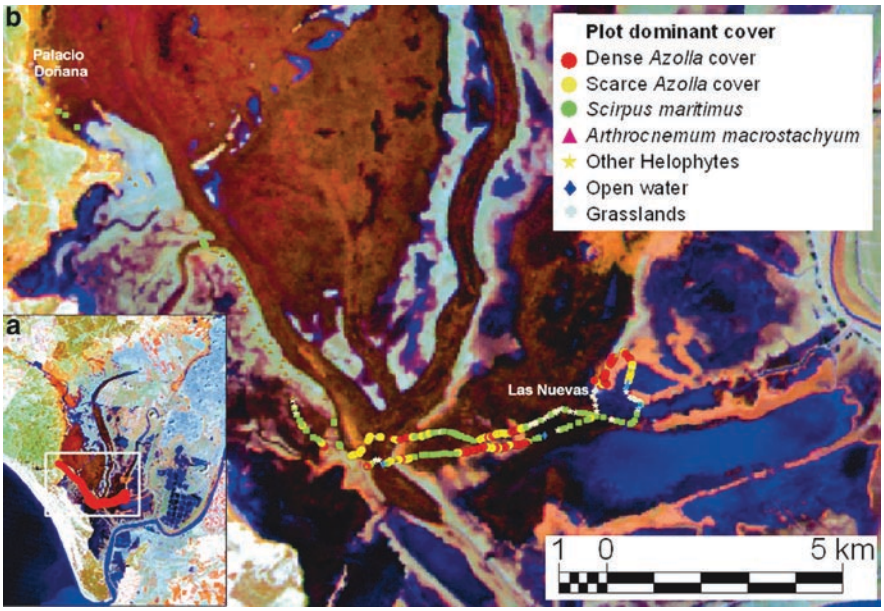

Fig. 31.5 (**a**) Landsat TM image of Doñana acquired on 5th May 2007 (false colour composite RGB bands 4-5-3) showing simultaneous to image acquisition ground-truth transect points (**b**) enlargement of sampled area showing the dominant species at each point. Densely covered *Azolla* points are clearly identified by *bright red circles*

Monitoring the Spread of an Aquatic Alien Species

The aquatic fern *Azolla filiculoides* is a small floating plant originally from America and largely naturalized in Northern Europe. Its physiology and growth pattern limits its access to light for the submerged vegetation.

Azolla tends to deplete phosphorous, generates anoxic bottoms under the dense carpets it forms, and prevents the development of other submerged or floating vegetation species. This pteridophyte was first detected in Doñana marshlands in 2000, and has been found recurrently during the flooding season, invading larger and larger areas. In Doñana it is invading open marshes (open water bodies), marshland covered by helophytes and macrophytes, "*lucios*" (shallow lagoons) and "*caños*" (old tidal water courses). As Doñana marshlands occupy up to 25 000 ha, that become virtually inaccessible when flooded, it is a difficult task to map *Azolla* distribution through conventional methods. This fern grows and spreads at the beginning of the flooding season (January) and finally dies off during the drying out period (from May to June).

Usually, the invaded wetlands appear fully covered and this modifies their reflective characteristics. The alien fern shows a characteristic spectral signature that is very different from the rest of aquatic plants, and this makes it possible to

map it even amid other dominant species such as *Scirpus litoralis*, *Scirpus maritimus* or *Arthrocnemum macrostachyum*. Since 2003, the LAST-EBD has been systematically collecting ground-truth data in Doñana marshlands, recording the presence and cover (%) of *Azolla* across transects simultaneously to Landsat TM and ETM+ acquisitions. Areas densely covered by *Azolla* appear in the images as highly reflective in the Near Infrared region (700–1,100 nanometers): this suggests high photosynthetic activity, much higher than that shown by native vegetation in flooded areas (Fig. 31.5).

Discussion

Traditional monitoring at the plot scale is strongly complemented by monitoring using remote sensing, as the latter provides information integrated at the landscape scale that can easily be combined with ground-truth data. While probes and sensors may be reporting local changes for a parameter, remote sensing images give the opportunity to extrapolate the information and quantitatively map the targeted variable and its gradients in a spatially explicit way. Underlying processes mapped at the landscape scale may reveal natural trends, induced changes, sudden threats or blooms, thus providing a valuable synoptic tool for adaptive wetlands management (Gardiner and Díaz-Delgado 2007). Furthermore, long time-series of images enhance long-term monitoring by helping to reconstruct historical processes that would otherwise remain uncertain. Retrospective mapping of synoptic parameters allows us to assess land cover changes in comparison to historical trends (anomalies from the average). Restoration projects may also benefit by using historical remote sensing images and the resulting maps as a baseline reference.

Landscape monitoring of Doñana marshlands is helping to integrate plot data on species richness, abundance, presence, water quality or breeding success with inundation level, annual hydroperiod or water turbidity. Other remote sensing monitoring protocols to be soon implemented will focus on: water temperature, evapotranspiration, net primary production, plant cover, and helophyte and macrophyte distribution mapping.

However, the techniques that we have implemented to monitor the processes mentioned above might not be easily extrapolated to other wetlands.

Specific characteristics of the Doñana marshlands have led us to apply specific and empirical remote sensing methods not necessarily valid for other wetlands. However, while there is likely to be a site-specific element to the development of protocols for other sites, many of the general approaches we have developed could be readily adapted elsewhere.

Acknowledgements This study was funded by the Doñana National Park administration (Spanish Ministry of Environment) through the research project "Reconstruction of bird population dynamics during the last three decades", by the Spanish Ministry of Science and Education through the research project HYDRA (# CGL2006-02247/BOS) and by help from the National Environmental Remote Sensing Network (# CGL2007-28828-E/BOS). Doñana National Park and Natural Park

provided permits for field work in protected areas with restricted access. A. Travaini, H. Le Franc, D. Paz, A. Polvorinos, C. Rodríguez, and I. Román helped with field work. J.C. Gilabert, J.L. Pecharromán, L. M. Campoy and P.L. Porta helped with image processing. The authors want also to thank Clive Hurford for reviewing the manuscript and for his suggestions to improve the readability of the chapter.

References

Ángel-Martínez MC (1994) Aplicación de la teledetección en la localización de superficies de agua. Unpublished CEDEX Technical Report, 120 pp

Baker C, Lawrence R, Montagne C, Patten D (2006) Mapping wetlands and riparian areas using landsat ETM+ imagery and decision-tree-based models. Wetlands 26:465–474

Barret EC, Curtis LF (1999) Introduction to environmental remote sensing, 3rd edn. London, Routledge 457 pp

Bustamante J, Pacios F, Díaz-Delgado R, Aragonés D (2009) Predictive models of turbidity and water depth in the Doñana marshes using Landsat TM and ETM+ images. J Environ Manage 90:2219–2225

Castaño S, Mejuto MF, Vela A, Quintanilla A, Ruiz JR (1999) Monitoring of wetlands evolution. In: Montesinos S, Castaño S (eds) Application of space techniques to the integrated management of river basin water resources (ASTIMwR). European Commission, Brussels, pp 27–49

Crist EP, Cicone RC (1984) A physically-based transformation of thematic mapper data: The TM Tasseled Cap. IEEE Trans Geosci Remote Sens GE-22:256–263

Díaz-Delgado R, Bustamante J, Pacios F, Aragonés D (2006a) Hydroperiod of Doñana marshes: Natural or anthropic origin of inundation regime? In: ESA & Ramsar Convention (eds) Proceedings of the 1st GlobWetland Symposium. 19–20 October, Frascatti, Italy

Díaz-Delgado R, Bustamante J, Aragonés D, Pacios F (2006b) Determining water body characteristics of Doñana shallow marshes through remote sensing. In: IGARSS 2006 (ed) IEEE international conference on geoscience and remote sensing symposium, July 31–August 4, Denver, pp 3662–3663

Domínguez Gómez JA (2002) Estudio de la calidad del agua de las lagunas de gravera mediante teledetección. PhD thesis, Alcalá de Henares, Universidad de Alcalá, 320 pp

Engman ET, Gurney RJ (1991) Remote sensing in hydrology. Chapman & Hall, London, 225 pp

Gardiner N, Díaz-Delgado R (2007) Trends in selected biomes, habitats and ecosystems: Inland waters. In: Strand H, Höft R, Strittholt J, Miles L, Horning N, Fosnight E (eds) Sourcebook on remote sensing and biodiversity indicators. Secretariat of the Convention on Biological Diversity, Montreal, pp 83–102

Kyu-Shun L, Tae-Hoon K, Yeo-Sang Y, Sang-Ming S (2001) Spectral characteristics of shallow turbid water near the shoreline on inter-tidal flat. Korean J Remote Sens 17:131–139

McFeeters SK (1996) The use of the Normalized Difference Water Index (NDWI) in the delineation of open water features. Int J Remote Sens 17:1425–1432

Ozesmi SL, Bauer ME (2002) Satellite remote sensing of wetlands. Wetlands Ecol Manage 10:381–402

Susskind J, Rosenfield J, Reuter D, Chahine M (1984) Remote sensing of weather and climate parameters from HIRS 2/MSU on TIROS-N. J Geophys Res Atmos 89:4677–4697